Endoplasmic reticulum stress influences the localization of prion protein in the small intestine and mesenteric lymph nodes

Erdal Balcan[1,*], Zübeyde Öztel[1] and Alexander Polevshchikov[2]

[1]*Manisa Celal Bayar University, Faculty of Arts and Science, Molecular Biology Section, Department of Biology*, 45030 Manisa, Turkey
[2]*Institute of Experimental Medicine*, Saint-Petersburg 197376, Russian Federation

*Corresponding author: erdal.balcan@cbu.edu.tr

Abstract: Tunicamycin is an endoplasmic reticulum (ER) stressor that inhibits protein glycosylation and promotes ER stress. To better understand the localization and traffic of prion protein (PrP) in both basal and ER stress conditions, we evaluated the presence and relative expression of PrP in the intestinal compartments of normal and tunicamycin-treated mice. After tunicamycin treatment, the level of PrP was significantly increased in enterocytes and blind-ended villous lymphatic vessels (lacteals), but was decreased in M cells. These results suggested that intake from the gut and transfer into lymphoid compartments of basal PrP occurs largely through the M cell-Peyer's patch-mesenteric lymph node axis, and also alternatively through the enterocyte-lacteal-mesenteric lymph node axis. In ER stress, the enterocyte-lacteal-mesenteric lymph node is the sole axis for PrP transmission. Results also indicated that germinal centers and high endothelial venules (HEVs) are the most prominent portal for entry of PrP in both basal and ER stressed conditions. We speculated that PrP may use alternative routes for entry into intestinal compartments according to the pathophysiological state and that the mechanism managing the routes of PrP could contribute to the development of new therapeutic strategies against prion diseases as well as ER stress-related intestinal disorders.

Keywords: prion protein, Peyer's patches, mesenteric lymph node, endoplasmic reticulum (ER) stress

INTRODUCTION

Conversion of the normal cellular isoform of the prion protein (PrP^c) into the abnormal and disease-associated isoform (PrP^{Sc}) is a major reason for the group of progressive neurodegenerative defects called transmissible spongiform encephalopathies (TSE) or prion diseases. PrP^c is a glycosylphosphatidylinositol (GPI)-anchored extracellular glycoprotein that has two *N*-linked glycosylation sites [1] and is widely expressed in various cell types in both neuronal and non-neuronal tissues [2]. Expression of PrP^c is essential for TSE susceptibility in both humans and animals [3] due to its ability to undergo conformational change to PrP^{Sc}. The involvement of the gastrointestinal system in the uptake of the TSE agent is widely accepted [4]. Ingested prion is absorbed through the gastrointestinal wall and accumulates in secondary lymphoid tissues prior to transmission to the central nervous

system (CNS). This route involves a process called neuroinvasion that is not yet fully understood. As a unique part of the intestinal immune system, M cells are responsible for the transepithelial transport of antigenic determinants [5] and are a strong candidate for migration of prion protein from gut lumen to Peyer's patches. They are specialized intestinal epithelial cells found in the follicle-associated epithelium (FAE) covering Peyer's patches that mediate transcytosis of intestinal antigenic determinants to downstream local dendritic cells through their sac-like structural organizations, the so-called M-cell pocket [6,7]. However, conflicting results have also been reported, and although a series of *in vitro* and *in vivo* studies have suggested that M cells are the potential entry point for prion protein [8-10], the detection of prion protein in enteroendocrine cells [11] and in vesicular endosomes of enterocyte surrounding Peyer's patches suggests an alternative route for prion ingestion beside M cell-

dependent uptake [12-14]. However, knowledge of the precise cellular mechanism involved in the transport of prion protein into secondary lymphoid tissues through intestinal Peyer's patches is still lacking. The prominent role of PrP in intestinal tissue is also not fully understood despite it being expressed in many intestinal compartments, such as the enteric nervous system and the lamina propria. Thus far, several studies have explored the relationships between PrP and cellular stress [15-19]. Although ER stress seems to be a transcriptional regulator for *PRNP* gene expression [20], what happens in the gut during ER stress is still a matter of debate.

Researchers have indicated that prion has a regulatory role in intestinal epithelial cellular junctions and that altered localization and deficiency of prion exacerbates inflammation, oxidative stress and intestinal barrier dysfunction, which are contributors to inflammatory bowel disease pathogenesis [21,22]. Furthermore, PrP has an anti-inflammatory and cytoprotective effect in dextran sodium sulphate (DSS)-induced colitis mice models [21]. However, basal intestinal permeability was not identified in wild-type, PrP-overexpressed or PrP^c-knockout mice [21], and no association between prion deficiency and increased tissue damage in response to DSS has been shown [23]. Therefore, in this study we investigated prion expression and the adjustment of prion levels during ER stress in mouse small intestine. By analyzing the intestinal route(s) of prion movement, we wanted to obtain an improved understanding of the effect of ER stress.

MATERIALS AND METHODS

Ethics statement

This study was approved by the Animal Experimentation Ethics Committee of the Medical School (Approval No. 77.637.435-70), Manisa Celal Bayar University, Manisa, Turkey. All experimental procedures were performed in accordance with the Helsinki Declaration and the Manisa Celal Bayar University Ethic Rules. A total of 18 Balb/c male mice aged 6-8 weeks were housed in a pathogen-free and environmentally controlled facility of the Research and Application Center for Laboratory Animals of Manisa Celal Bayar University, Manisa, Turkey, according to the ethical rules of the Animal

Experimentation Ethics Committee of the Medical School. The number of animals was limited to 10 (5 tunicamycin-treated and 5 control) in order to reduce the number of animals exposed to suffering.

Induction of ER-stress

To initiate ER stress in mice (n=5), tunicamycin (Sigma, T7765), a potent protein *N*-glycosylation inhibitor, was administered intraperitoneally (i.p.) at a single dose of 1 µg/g body weight for 24 h. The same volume of 0.9% NaCl was injected to the control group (n=5). After 24 h, the mice were killed by cervical dislocation and ileal regions of the small intestines and mesenteric lymph nodes were rapidly harvested. Sections of the removed tissues were stored at -80°C for Western blotting analysis.

Immunohistochemical and immunofluorescence analyses

Tissue sections were fixed in 10% neutral buffered formalin for 24 h and dehydrated prior to paraffin embedding. The tissue sections were 5 mm thick and mounted on poly-*L*-lysine-coated slides. After deparaffinization in xylene, rehydration in graded ethanol solutions and washing with phosphate-buffered solution (PBS, pH 7.5), sections were immersed in 10 mM citrate buffer (pH 6.0) for 20 min in a 96°C water bath, followed by a 20 min cool-down period implemented for antigen retrieval. Endogenous peroxidase activity was blocked by 3% H_2O_2 diluted in absolute methanol for 10 min at room temperature. Following blocking with IHC Select Q Blocking Reagent (Millipore, Cat # 20773) for 30 min at 37°C, the tissue sections were incubated with primary mouse anti-PrP antibody (clone G-12; specific for an epitope mapped between amino acids 217-232 near the C-terminus of PrP of human origin, (SantaCruz, sc398451), at a dilution of 1:200 in PBS containing 3% bovine serum albumin (BSA) overnight at +4°C, prior to incubation with horseradish peroxidase (HRP)-conjugated secondary antibody (goat anti-Mouse IgG-H&L; Abcam, ab97040), diluted 1:400 in 3% BSA in PBS for 90 min at room temperature. To visualize the tunicamycin-treated ER stress, rabbit anti-ATF6 primer antibody (Abcam, UK; ab203119) and HRP-conjugated goat anti-Rabbit IgG-H&L (Abcam, ab7090) secondary

antibody were used. Immunohistochemical reactivity was visualized by 3.3'-diaminobenzidine (DAB) (Vector Laboratories, USA; Cat # SK-4100). Finally, counterstaining of slides was performed using methyl green. Immunofluorescence analysis was performed with the same primary antibody diluted 1:400 in incubation buffer: 1% BSA, 1% donkey serum and 0.3% Triton X-100 in PBS) overnight at +4°C. After three washes in PBS, the bound antibody was visualized by incubation with a fluorescein isothiocyanate (FITC) conjugated secondary antibody (Goat Anti-Mouse IgG H&L; Abcam, ab7064) (1:400 dilution) for 1 h at room temperature in a dark and humid chamber. Nuclear staining was performed with 4'6-diamidino-2-phenylindole (DAPI) (Santa Cruz, USA; sc3598) at 1:1000 dilution in McIlvaine's buffer).

Western blotting

To extract proteins from ileal tissues, homogenization was performed in radioimmunoprecipitation assay (RIPA) buffer containing 1 mM phenylmethanesulfonyl fluoride (PMSF) (Sigma, USA.; D7626) and a protease inhibitor cocktail (30 μL per g tissue) (Sigma, P8340). Protein concentrations were calculated using a bicinchoninic acid (BCA) assay kit (Pierce BCA Protein Assay Kit, Thermo Scientific, Rockford, Illinois, USA) according to the manufacturer's instructions; protein extracts were boiled in 0.8 M Tris-HCl, 10% glycerol, 20% β-mercaptoethanol, 10% sodium dodecyl sulfate (SDS), 0.02% bromophenol blue at 96°C for 4 min. Equal amounts of protein (10 μg) containing samples were loaded onto 4-7.4% polyacrylamide gels and electrophoresis was performed at 15 mA for 2 h at room temp using a Mini Protean electrophoresis apparatus (Bio-Rad, Hercules, California, USA). Western blot analysis was conducted according to standard procedure. Briefly, proteins were transferred onto polyvinylidene fluoride (PVDF) membranes overnight at 30 mA using a Mini Trans Blot System (Bio-Rad, Hercules, California, USA). PVDF membranes were blocked with non-fat dried milk (Sigma, M7409) (5% w/v) in Tris-buffered saline containing Tween 20 (TBST; 0.1% vol/vol) for 30 min prior to probing with primary anti-PrP antibody, diluted 1:400 in 3% BSA in TBST for 1 h at room temp. After washing in TBS-T, the membranes were incubated with secondary horseradish peroxidase (HRP)-conjugated antibody (1:400

dilution) for 1 h. DAB was used as chemiluminescence substrate for visualization of immunoreactive protein bands. Glyceraldehyde 3-phosphate dehydrogenase (GAPDH) (Abcam, ab8245) was used as housekeeping protein and at a similar dilution.

Quantification and statistical analysis

The number of PrP-positive cell and DAB-positivity were scored for the small intestine and mesenteric lymph node and expressed as the percentage of cell positivity and DAB intensity in both control and tunicamycin-treated groups. Randomly selected digital images were loaded to ImageJ (https://imagej.nih.gov/ij/; ver.1.52) and the percentage of cell positivity and DAB intensity were obtain using "cell counter" and "IHC profiler macro" plugins, respectively. For quantification of Western blot data, a standard plot analysis algorithm of ImageJ was used. All statistical differences between control and ER-stressed groups were performed by two-tailed Student's t-test, with $P<0.05$ as the level of statistically significant difference (IBM SPSS software, version 22.0, SPSS Inc., Chicago, IL, USA).

RESULTS

### Immunohistochemical analysis of PrP in villus compartments of control mice

Some of the small intestinal villous enterocytes in control mice showed PrP immunoreactivity (Fig. 1A). PrP accumulation was restricted to the enterocytes located at the tips of villi, showing a cytosolic distribution in these cells (Fig. 1B, C). Other intestinal epithelial cells, goblet cells, intraepithelial lymphocytes of the brush border zone and infiltrating lymphocytes of lamina propria were negative for PrP in control mice (Fig. 2A-C). Similar results were also observed in Paneth cells (Fig. 2B). However, PrP accumulation was evident in the lacteals of the lamina propria (Fig. 2D).

Immunohistochemical analysis of PrP in Peyer's patches of control mice

PrP was abundant in some lymphatic cells in the germinal centers of Peyer's patches in control mice (Fig. 3A-C). Weak PrP accumulation was evident in the basal
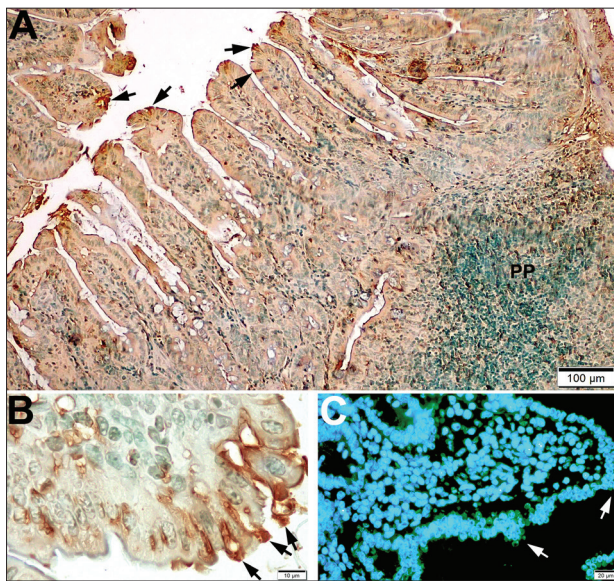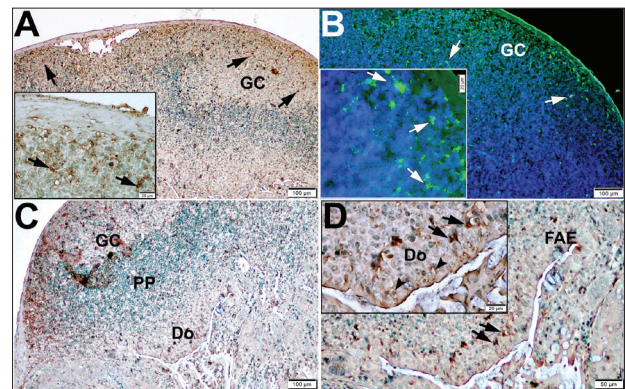
Fig. 1. Immunohistochemistry and immunofluorescence staining of PrP in villus compartments of control mice. **A, B** – Immunoreactivity in villus tips. **C** – Immunofluorescence staining of villi (merged image, of nuclei stained with DAPI). Arrows indicate a positive reaction for PrP. PP – Peyer's patch.
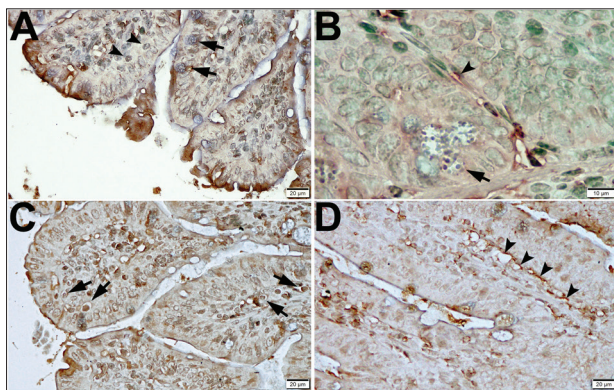
Fig. 2. Immunoreactions in the intestinal cells of control mice. **A** – Goblet cells (arrows) and intraepithelial lymphocytes (arrowheads). **B** – Paneth cells (arrow) and intestinal epithelial cells (arrowhead). **C** – Infiltrating lymphocytes (arrows). **D** – Lacteals (arrowheads).

regions of M cells in the follicle-associated epithelium (FAE) surrounding the dome area of Peyer's patches (Fig. 3D). These results indicated that, apart from M cells of the FAE, enterocytes that occupied the tips of the villi are responsible for internalization of PrP as well under basal conditions. Although we could not identify any reaction in the nerve-like structures of the Peyer's patch follicles, their associated enteric nervous system ganglia and mesothelium were positive for PrP (not shown).

Fig. 3. Distribution of PrP reactions in Peyer's patches of control mice. **A** – Immunohistochemical view of PrP in germinal centers (arrows). **B** – Immunofluorescence staining of germinal centers (white arrows). **C** – Positively stained M cells in the dome area (arrows). **D** – High power view of dome area in C. Arrowheads in inset of D point to other cells of follicular-associated epithelium. PP – Peyer's patch, GC – Germinal center, Do – Dome area, FAE – Follicle-associated epithelium.

PrP Immunohistochemistry in villus compartments of tunicamycin-treated mice

After induction of the ER stress, PrP staining intensity was strongly increased in the apical sides of enterocytes located in the villus (P=0.007; Supplementary Table S1, Fig. 4A-F), but the percentage of PrP-positive enterocytes was almost similar to those in the control (P=0.543) (Supplementary Table S1, Fig. 4E). A similar DAB intensity was also detected in the lacteals of the tunicamycin group (P=0.013; Supplementary Table S2, Fig. 4F). To visualize tunicamycin-treated ER stress, we used a monoclonal antibody specific for activating transcription factor 6 (ATF6) that activates the unfolded protein response (UPR) target genes during the ER stress. In tunicamycin-treated mice, ATF6 expression levels significantly increased in the small intestine when compared with the control (Supplementary Fig S1A, B). Interestingly, in the apical region of the enterocytes, the expression and cytosolic distribution of the ATF6 molecule appeared to be similar to that of PrP (Fig. 4, Supplementary Fig. S1A, B). This data suggests that the accumulation of PrP increased in villous enterocytes subjected to ER stress and that the lacteals could play a critical role in the transport of PrP into lymphoid compartments of the small intestine and to the mesenteric lymph node. Moreover, intraepithelial lymphocytes, stromal cells surrounding
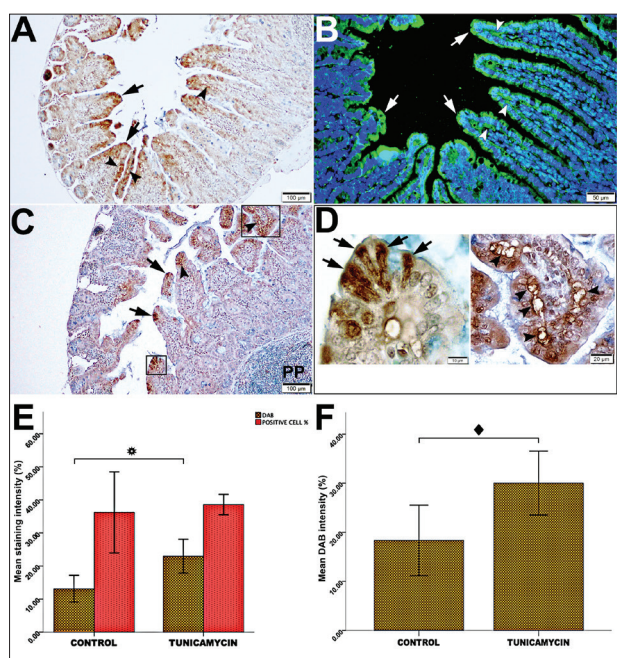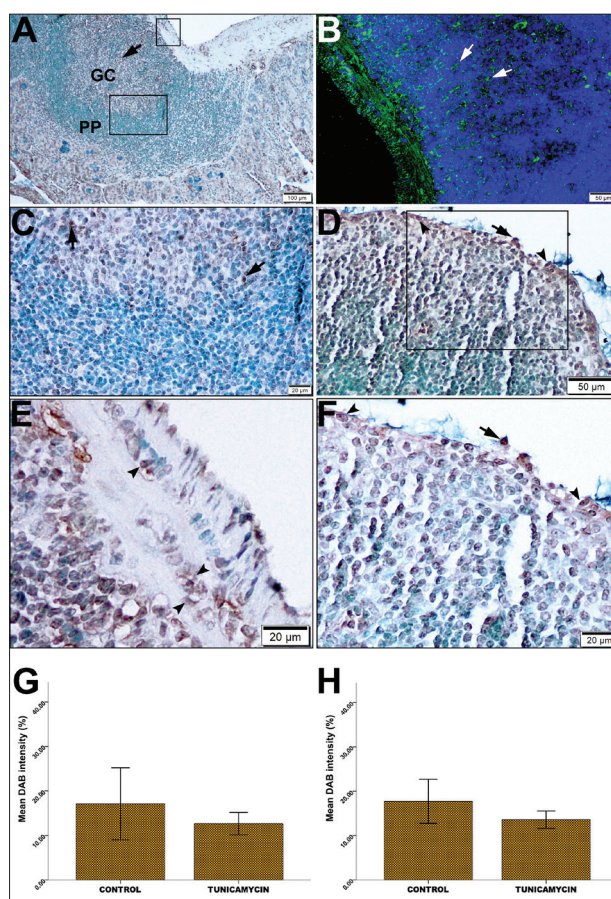
Fig. 4. Immunohistochemistry and immunofluorescence of PrP in villus compartments of tunicamycin treated mice. **A** – Immunohistochemical expression of PrP in villus tips (arrows) and lacteals (arrowheads). **B** – Immunofluorescence staining of villus tips (arrows) and lacteals (arrowheads), merged image; DAPI used as a counterstain for nuclei. **C** – Increased DAB signal in enterocytes (arrows) and lacteals (arrowheads). **D** – High power view of boxed areas in C. **E** – Histogram statistics of the differences in percentage of DAB positivity (brown columns) and percentage of PrP-positive enterocyte number (red columns) between control and tunicamycin-treated mice; star – statistically significant difference. **F** – Percentage of DAB intensity for lacteals; diamond – significant difference in lacteals. PP – Peyer's patch.

the crypts of Lieberkühn and the endothelial lining cells of the microcapillary system of the lamina propria were also positive for PrP in ER stress-induced mice. (Several PrP positive cells in the crypts of Lieberkühn were also detected (not shown), and according to their localization, these cells most likely are intestinal stem cells, but this needs to be confirmed).

PrP Immunohistochemistry in Peyer's patches of tunicamycin-treated mice

The intensity of PrP staining was relatively decreased in Peyer's patches in tunicamycin-treated mice (P=0.298; Supplementary Table S3, Fig. 5A-C, G). Weak accumulation of PrP was observed only in M cells, but other cell types in the FAE, including enterocytes and/or a limited number of goblet cells exhibited negative expression

Fig. 5. Immunohistochemistry and immunofluorescence of PrP in Peyer's patches of tunicamycin-treated mice. **A** – Decreased immunoreactivity of PrP in germinal centers (arrow indicates positive reactions). **B** – Decreased fluorescence signals in germinal centers (white arrows indicate positive signals); merged image. **C** – High magnification of germinal center in A (larger box). **D** – Decreased distribution of PrP in the dome area. Arrows and arrowheads – positive and negative cells, respectively. **E** – High magnification of enteric nervous system in A (smaller box). **F** – High magnification of boxed area in D. **G** – histogram statistics of DAB intensity in Peyer's patches. **H** – Histogram statistics of DAB intensity in the enteric nervous sytem. GC – germinal center, PP – Peyer's patch.

(Fig. 5D, F). Furthermore, PrP was detected within the ganglia of the enteric nervous system in both control and ER stress-induced mice, but decreased after the tunicamycin treatment (P=0.088; Supplementary Table S4, Fig.5 E, H). The finding of reduced expression of PrP within the ganglia of the enteric nervous system in tunicamycin-treated mice as compared to control mice suggests that neuroinvasion of PrP follows an alternative route in ER stress.

Immunohistochemistry of mesenteric lymph nodes

The most prominent differences between control and tunicamycin-treated mice were increased expression levels of PrP in the enterocytes and lacteals of ER-stressed intestines. In addition, ATF6 levels were also increased in the mesenteric lymph nodes after the tunicamycin treatment (Supplementary Fig. S1C, D). These results motivated us to investigate the transmission of PrP into mesenteric lymph nodes through enterocytes and lacteals at basal conditions. As expected, PrP was localized in germinal centers in both control and tunicamycin-treated mesenteric lymph nodes. In control mice, the PrP signal was observed in follicular dendritic cells of germinal centers and HEVs, but not in tingible body macrophages (Supplementary Fig. S2). In tunicamycin-treated mice, a large number of PrP-positive follicular dendritic cells that form a fibrillar network was observed in the germinal centers (Fig. 6A, B), but the intensity of PrP staining was moderately increased in these regions (P=0.139; Supplementary Table S5, Fig. 6A, B, G). PrP immunoreactivity (P=0.005) and the percentage of PrP-positive cells (P<0.001) in the HEVs of tunicamycin-treated mice were significantly increased when compared with control HEVs (Supplementary Table S6, Fig. 6C-F, H). PrP was also detected in medullary sinuses lining the endothelial cells (lymphatic endothelial cells (LECs)) in control mice, but signal intensity was moderately decreased after the tunicamycin treatment (not shown). These results suggest that internalization and transport of basal PrP into mesenteric lymph nodes occurs through different pathways in control and tunicamycin-treated mice. It seems that PrP internalization largely occurs through M cells of the dome region covering Peyer's patches in control mice whereas in tunicamycin-treated mice, the PrP route into mesenteric lymph nodes consists of enterocytes and villous lymphatic vessels (lacteals).
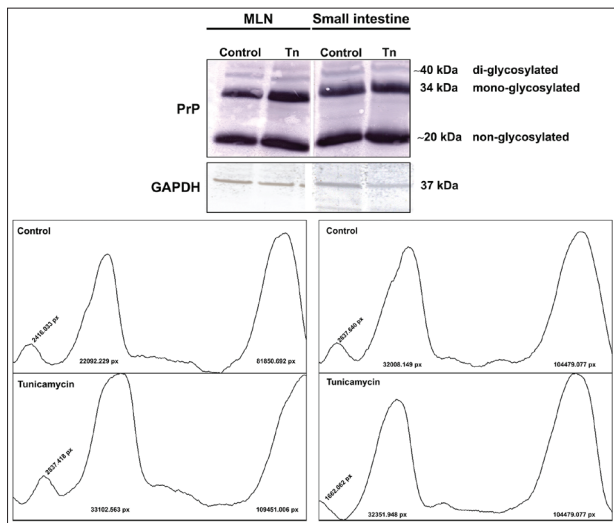
Western blot analysis

Although variable PrP expression profiles were observed in different localizations of the small intestine and mesenteric lymph nodes in both control and tunicamycin-treated mice, Western blot analysis of total tissues from the two groups did not reveal significant differences in the intensity of PrP expression
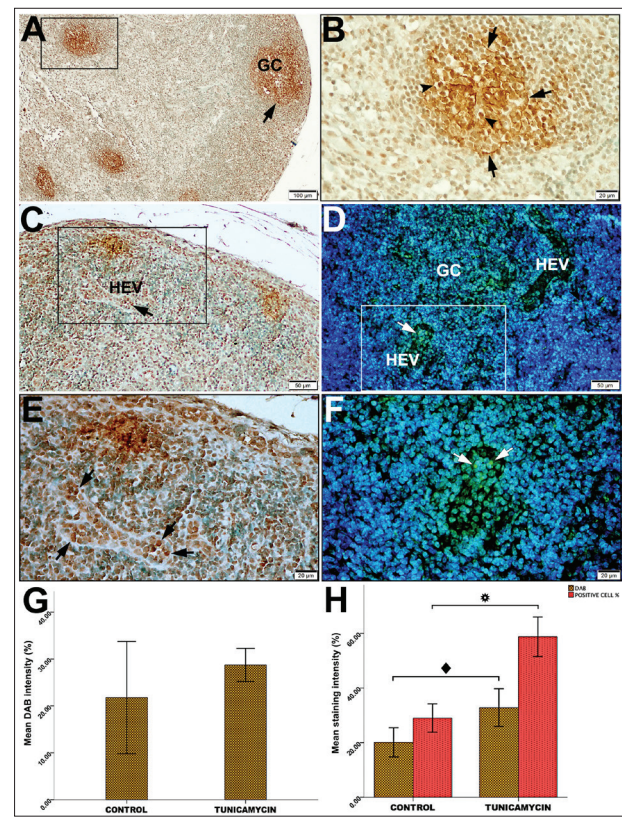
Fig. 6. Immunohistochemistry and immunofluorescence of PrP in mesenteric lymph nodes after tunicamycin treatment. **A** – Intense positivity for PrP in the fibrillar network of germinal centers and HEVs (arrows). **B** – High power view of the boxed area in A; arrowheads – macrophages stained with PrP antibody. **C** – DAB reactions for HEVs (arrow). **D** – Fluorescence signals for HEVs (arrow). **E** – High-power magnification of boxed area in C; arrows – PrP-positive cells in the HEV wall. **F** – High-power magnification of the boxed area in D; white arrows – PrP-positive cells in the HEV wall. **G** – Histogram statistics of germinal center distribution of PrP in DAB-stained tissue sections from two representative groups (P=0.139). **H** – Histogram statistics of DAB intensity and the percentage of positive cells in HEVs; (the P values were =0.005 and <0.001, indicated with a diamond and star, respectively). HEV – high endothelial venule, GC – Germinal center.

(Fig. 7). The PrP-specific signal of total tissue extracts was observed as a three-banded fraction pattern at ~20, 34 and ~40 kilodaltons corresponding to non-, mono- or diglycosylated forms, respectively. Strikingly, the band at the ~40 kDa region was very weak for a PrP signal, suggesting that PrP entered and was transported in a non- and/or monoglycosylated form in the mesenteric lymph nodes.

Fig. 7. Western blot analysis of tissue extracts from two groups showing three immunoreactive bands. Upper panel – di-, mono- and non-glycosylated forms of PrP at 40, 34 and 20 kDa, respectively. Lower panel – histogram plots of the relative densities of the obtained bands. No significant changes in total PrP levels between the two groups were observed (Tn – tunicamycin).

DISCUSSION

The proper functioning of a cell relies on the functional stability of its ER. As a crucial part of the digestive system, the small intestine has the widest surface for absorption of nutrients. Therefore, deterioration in the ER can be harmful for intestinal integrity and results in an inflammatory response in the host organism [24]. Given that the small intestine has an essential role in immune surveillance, the intestinal barrier function is crucial, especially for blocking foodborne exogenous pathogens and/or antigens [25,26], such as the prion, a proteinaceous infectious agent devoid of nucleic acid. Although a number of investigations have reported the role of PrP[c] in prion disease, uptake and transmissions of this molecule into the CNS remain still poorly understood. The general view is that secondary lymphoid tissues are the first cluster sites of prions before they are transmitted to the CNS [27,28]. Reports have shown that scrapie prion accumulates first in Peyer's patches and mesenteric lymph nodes after oral inoculation [29,30]. It was suggested that in this process, M cells of the dome region covering Peyer's patches act as an endocytic receptor because they express PrP[c] on their surfaces [31]. During the mucosal immune response, M cells take up luminal antigens and deliver them to dendritic cells through their sac-like structures, which are formed by invagination of the basal cell membrane [32]. In agreement with these data, we observed weak PrP expression in the basal regions of M cells in control mice. Since we did not determine dendritic cells because of the basal localization of low levels of PrP in M cells, we assumed that dendritic cells might be responsible for PrP migration into Peyer's patches, in agreement with previous data [33,34]. In addition to M cells, our study showed that villous enterocytes, which are responsible for nutrient absorption, are also responsible for basal PrP intake but the number and cellular localization of enterocytes expressing PrP in the control group was distinctly different from that in tunicamycin-treated mice. It has been reported that PrP is expressed in the villus and crypt epithelium [35,36], and it was also reported that PrP can be observed as weak apical granules within enterocytes [35]. These results appear to be consistent with our research that established that PrP is expressed on enterocytes located on the tips of the villi in both control and tunicamycin-treated mice. Meanwhile, apical PrP accumulations were strongly increased within the enterocytes in ER stress. However, we could not explain why PrP expression was restricted to only a few enterocytes that localized on the tips of villi or why these molecules displayed apical localizations in enterocytes.

The reasons why PrP expression is restricted to only a few enterocytes that localized on the tips of villi and why PrP exhibited apical localizations in enterocytes remain unknown. However, we speculate that these cells might be a powerful candidate for uptake of basal PrP from the gut lumen, in common with a previous study of the bovine spongiform encephalopathy agent [37]. Intriguingly, after the tunicamycin treatment, the increased PrP signal was also detected in the lacteals. The lacteals are intestinal partners that are responsible for the transmigration of PrP into mesenteric lymph nodes under pathophysiological circumstances such as ER stress. Previous results which reported that the disease-related form of PrP was transported from enterocytes into lacteals [12] would confirm this assumption, however, further research is required to better understand the interface between the enterocyte and lacteal. For instance, ER stress could induce an impairment of the intestinal barrier [38,39] so that enterocytes with disrupted cellular connections would allow the PrP to penetrate through from gut lumen into

lacteals. However, our results showed that PrP accumulation occurred along the apical side of enterocytes. We assumed that in response to ER stress, PrP-specific apical transporter(s) increase on enterocytes, or that transport of PrP from the gut lumen into lacteals occurs by transcytosis in the same way as M cells [10].

The high expression of PrP on the M cell apical surface has been reported [31]. It was also suggested that PrP is a potential antigen receptor for M cells and that this cell type could play a crucial role in prion disease [32]. However, other authors reported conflicting results, and no PrP reactivity on the M cell surface was suggested by the Miyazawa et al. [36], in line with Ford et al. [35]. The finding that ER stress induced PrP intake through enterocytes located in villus tips was unexpected and we concluded that the route of PrP entry is along the M cell-Peyer's patch axis to the intestinal villus enterocyte-lacteal axis during the ER stress. Accordingly, weak immunostained M cells were observed in the control group, but this reactivity was greatly decreased in stressed mice. However, we could not explain how ER stress contributed to this change and which molecular mechanism underlies this phenomenon remains a mystery and requires further study. Although enterocytes have been reported to have no phagocytic activity and are not specialized for transcytosis [40], it is known that clathrin-coated vesicles are major cellular components for transcytosis of some nutrients such as vitamin B12 in enterocytes [41].

In the small intestinal villi, lacteals stream into the lymphatic network and the afferent lymphatic capillaries of mesenteric lymph nodes [42]. As a compartment of the gut immune surveillance machinery, the lacteal provides a space for immune cell infiltration [43]. In addition to this drainage channel, lacteals may have a key role in pathological situations such as inflammatory bowel disease, as was reported recently [44,45]. As mentioned above, the lacteals can also provide a transport route for basal PrP under physiological conditions as well as in response to ER stress. Similar to our results, disease-related PrP was observed in the lacteals in a sheep model but not in the dome of Peyer's patches [46]. Close contacts between lacteals and nerve endings have been reported [47,48], however the functional significance of this interplay remains poorly understood.

In our experiments, PrP expression was evident in some lymphatic cells in the germinal centers of Peyer's patches in control mice. This finding is consistent with previous reports that showed the early accumulation of orally inoculated prions in Peyer's patches as well as in mesenteric lymph nodes [36]. However, in ER stress, the accumulation of PrP in Peyer's patches was strongly decreased.

The wide distribution of PrP in the small intestine and its immune system-related compartments both in control and ER-stressed mice suggest that this molecule uses different routes and targets that are specialized according to the pathophysiological state in these intestinal sites. Hence it is possible that it serves as a regulator for various cellular events related to nutrient absorption and host defense mechanisms.

Cross-talk between the mesenteric lymph nodes and small intestine is essential for the control of development and differentiation of adaptive immune system cells [49]. PrP localizations in mesenteric lymph nodes in control and stressed mice were described in previous studies [35]. HEVs were responsible for PrP[Sc] incorporation in mesenteric lymph nodes [50] in the absence of follicular dendritic cells (FDC). However, the predominant accumulation sites of PrP were follicular dendritic cells of the germinal center [35]. Together with the germinal centers, we observed increased PrP immunoreactivity in the HEV wall of stressed mice, suggesting that HEV may be an alternative portal for PrP not only in the absence of FDC, but also in the presence of these cells. In ER-stressed mice, the levels of PrP increased when compared to the control, suggesting that during the pathophysiological state, the major accumulation and neuroinvasion site is the FDC.

Western blots of the tissues from each group did not reveal clear differences in the intensity of the PrP-specific signal. PrP shows three different glycosylation forms, non-, mono- or diglycosylated with different molecular weights, depending on the number of glycosylation sites in its two *N*-linked oligosaccharide chains [51]. The observation that control and tunicamycin-treated mice had similar band intensities at ~20 and 34 kDa, but not at ~40 kDa was unexpected because tunicamycin is an *N*-linked glycosylation inhibitor. These results suggest that PrP molecules from the small intestine and mesenteric lymph node escaped the effect of tunicamycin (*N*-glycosylation inhibition), as was previously reported in different *in vitro* models [52]. Although we were unable to detect the glycosylation profile of PrP after
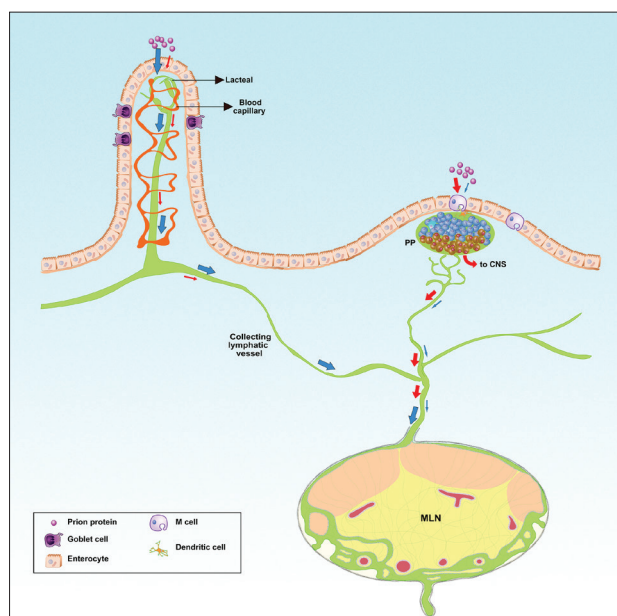
Fig. 8. According to immunohistochemistry and immunofluorescence findings, PrP intake from the gut lumen and transport to the intestinal lymphoid parenchyma and then to the mesenteric lymph node depends on the stress conditions. Our results suggest that in ER stress, the route of basal PrP movement is largely through the enterocyte-lacteal-mesenteric lymph node axis (cyan arrows). Under physiological conditions, PrP reaches the CNS *via* the M cells-Peyer's patches (PP)-enteric ganglia (red arrows) route. However, this hypothesis needs confirmation. CNS – central nervous system, MLN – Mesenteric lymph node.

tunicamycin treatment, it could be argued that non- and/or monoglycosylated forms of PrP were absorbed from gut lumen and transported into intestinal compartments and mesenteric lymph nodes. This is in partial agreement with a previous experimental report indicating that *N*-linked glycans are not required for intracellular trafficking of PrP [53]. Therefore, the functionality of *N*-linked glycans of PrP in the intake and transport of this molecule remains unexplained and further investigations are needed to clarify the role of the glycosylation apparatus for intake of PrP and its transfer to intestinal compartments and mesenteric lymph nodules in both normal and pathophysiological circumstances.

In conclusion, we demonstrated that in ER stress, the intake of PrP from the gut lumen and its transfer to the intestinal compartment as well as mesenteric lymph nodes occurs through a different route from the M cell-dependent pathway. This is summarized in Fig. 8. Moreover, our results implied that the glycosylation

status of PrP does not interfere with the movement of this molecule to intestinal lymphoid compartments and mesenteric lymphoid sites, even in ER stress. Recent studies have linked PrP and barrier-forming cellular interactions in intestinal epithelial cells [22]. It was postulated that the disruption of several desmosomal components of the intestinal epithelium impairs barrier function and thereby contributes to the pathogenesis of intestinal disorders such as inflammatory bowel disease [22]. Similarly, ER stress in the intestinal epithelial cells also activates the host immune response and induces inflammatory bowel disease [39]. In this study, a striking difference between control and ER-stressed mice was revealed as regards the absorption and transfer of PrP into intestinal lymphoid sites and mesenteric lymph nodes. Finally, the elucidation of the underlying mechanisms that control the PrP route during pathophysiological states will contribute towards the development of new strategies against prion diseases, as well as intestinal disorders such as inflammatory bowel disease.

Author contributions: EB carried out the experiments, the data collection, Western blotting assays, quantitative statistical analyses and participated in manuscript preparation. ZO carried out the IHC and IF assays and participated in the design of the study. AP contributed to the literature review, manuscript preparation and revision, and participated in the design and coordination of the study.

Conflict of interest disclosure: The authors declare no conflict of interest.

REFERENCES

1. Pastore A, Zagari A. A structural overview of the vertebrate prion proteins. Prion. 2007;1(3):185-97.
2. Sakudo A, Onodera T, Suganuma Y, Kobayashi T, Saeki K, Ikuta K. Recent advances in clarifying prion protein functions using knockout mice and derived cell lines. Mini Rev Med Chem. 2006;6(5):589-601.
3. Bueler H, Aguzzi A, Sailer A, Greiner RA, Autenried P, Aguet M, Weissmann C. Mice devoid of PrP are resistant to scrapie. Cell. 1993;73(7):1339-47.
4. Beekes M, McBride PA. Early accumulation of pathological PrP in the enteric nervous system and gut-associated lymphoid tissue of hamsters orally infected with scrapie. Neurosci Lett. 2000;278(3):181-4.
5. Neutra MR, Frey A, Kraehenbuhl JP. Epithelial M cells: gateways for mucosal infection and immunization. Cell. 1996;86(3):345-8.

6. Brandtzaeg P, Kiyono H, Pabst R, Russell MW. Terminology: nomenclature of mucosa-associated lymphoid tissue. Mucosal Immunol. 2008;1(1):31-7.

7. Kraehenbuhl JP, Neutra MR. Epithelial M cells: differentiation and function. Annu Rev Cell Dev Biol. 2000;16:301-32.

8. Donaldson DS, Kobayashi A, Ohno H, Yagita H, Williams IR, Mabbott NA. M cell-depletion blocks oral prion disease pathogenesis. Mucosal Immunol. 2012;5(2):216-25.

9. Donaldson DS, Sehgal A, Rios D, Williams IR, Mabbott NA. Increased Abundance of M Cells in the Gut Epithelium Dramatically Enhances Oral Prion Disease Susceptibility. PLoS Pathog. 2016;12(12):e1006075.

10. Heppner FL, Christ AD, Klein MA, Prinz M, Fried M, Kraehenbuhl JP, Aguzzi A. Transepithelial prion transport by M cells. Nat Med. 2001;7(9):976-7.

11. Davies GA, Bryant AR, Reynolds JD, Jirik FR, Sharkey KA. Prion diseases and the gastrointestinal tract. Can J Gastroenterol. 2006;20(1):18-24.

12. Jeffrey M, Gonzalez L, Espenes A, Press C.M, Martin S, Chaplin M, Davis L, Landsverk T, MacAldowie C, Eaton S, McGovern G. Transportation of prion protein across the intestinal mucosa of scrapie-susceptible and scrapie-resistant sheep. J Pathol. 2006;209(1):4-14.

13. Kujala P, Raymond CR, Romeijn M, Godsave SF, van Kasteren SI, Wille H, Prusiner SB, Mabbott NA, Peters PJ. Prion uptake in the gut: identification of the first uptake and replication sites. PLoS Pathog. 2011;7(2): e1002449.

14. Mishra RS, Basu S, Gu Y, Luo X, Zou WQ, Mishra R, Li R, Chen SG, Gambetti P, Fujioka H, Singh N. Protease-resistant human prion protein and ferritin are cotransported across Caco-2 epithelial cells: implications for species barrier in prion uptake from the intestine. J Neurosci. 2004;24(50):11280-90.

15. Hetz C, Castilla J, Soto C. Perturbation of endoplasmic reticulum homeostasis facilitates prion replication. J Biol Chem. 2007;282(17):12725-33.

16. Roffe M, Beraldo FH, Bester R, Nunziante M, Bach C, Mancini G, Gilch S, Vorberg I, Castilho BA, Martins VR, Hajj GN. Prion protein interaction with stress-inducible protein 1 enhances neuronal protein synthesis via mTOR. Proc Natl Acad Sci U S A. 2010;107(29):13147-52.

17. Misiewicz M, Dery MA, Foveau B, Jodoin J, Ruths D, LeBlanc AC. Identification of a novel endoplasmic reticulum stress response element regulated by XBP1. J Biol Chem. 2013;288(28):20378-91.

18. Gao Z, Peng M, Chen L, Yang X, Li H, Shi R, Wu G, Cai L, Song Q, Li C. Prion Protein Protects Cancer Cells against Endoplasmic Reticulum Stress Induced Apoptosis. Virol Sin. 2019;34(2):222-34.

19. Orsi A, Fioriti L, Chiesa R, Sitia R. Conditions of endoplasmic reticulum stress favor the accumulation of cytosolic prion protein. J Biol Chem. 2006;281(41):30431-8.

20. Dery MA, Jodoin J, Ursini-Siegel J, Aleynikova O, Ferrario C, Hassan S, Basik M, LeBlanc AC. Endoplasmic reticulum stress induces PRNP prion protein gene expression in breast cancer. Breast Cancer Res. 2013;15(2):R22.

21. Martin GR, Keenan CM, Sharkey KA, Jirik FR. Endogenous prion protein attenuates experimentally induced colitis. Am J Pathol. 2011;179(5):2290-301.

22. Petit CS, Barreau F, Besnier L, Gandille P, Riveau B, Chateau D, Roy M, Berrebi D, Svrcek M, Cardot P, Rousset M, Clair C, Thenet S. Requirement of cellular prion protein for intestinal barrier function and mislocalization in patients with inflammatory bowel disease. Gastroenterology. 2012;143(1):122-32.

23. Petit CS, Besnier L, Morel E, Rousset M, Thenet S. Roles of the cellular prion protein in the regulation of cell-cell junctions and barrier function. Tissue Barriers. 2013;1(2):e24377.

24. Ma X, Dai Z, Sun K, Zhang Y, Chen J, Yang Y, Tso P, Wu G, Wu Z. Intestinal Epithelial Cell Endoplasmic Reticulum Stress and Inflammatory Bowel Disease Pathogenesis: An Update Review. Front Immunol. 2017;8:1271.

25. Menard S, Cerf-Bensussan N, Heyman M. Multiple facets of intestinal permeability and epithelial handling of dietary antigens. Mucosal Immunol. 2010;3(3):247-59.

26. Santaolalla R, Fukata M, Abreu MT. Innate immunity in the small intestine. Curr Opin Gastroenterol. 2011;27(2):125-31.

27. Heggebo R, Press CM, Gunnes G, Inge Lie K, Tranulis MA, Ulvund M, Groschup MH, Landsverk T. Distribution of prion protein in the ileal Peyer's patch of scrapie-free lambs and lambs naturally and experimentally exposed to the scrapie agent. J Gen Virol. 2000;81(Pt9):2327-37.

28. Klein MA, Frigg R, Flechsig E, Raeber AJ, Kalinke U, Bluethmann H, Bootz F, Suter M, Zinkernagel RM, Aguzzi A. A crucial role for B cells in neuroinvasive scrapie. Nature. 1997;390(6661):687-90.

29. Mabbott NA, Bruce ME. Prion disease: bridging the spleen-nerve gap. Nat Med. 2003;9(12):1463-4.

30. Prinz M, Huber G, Macpherson AJ, Heppner FL, Glatzel M, Eugster HP, Wagner N, Aguzzi A. Oral prion infection requires normal numbers of Peyer's patches but not of enteric lymphocytes. Am J Pathol. 2003;162(4):1103-11.

31. Nakato G, Hase K, Suzuki M, Kimura M, Ato M, Hanazato M, Tobiume M, Horiuchi M, Atarashi R, Nishida N, Watarai M, Imaoka K, Ohno H. Cutting Edge: Brucella abortus exploits a cellular prion protein on intestinal M cells as an invasive receptor. J Immunol. 2012;189(4):1540-4.

32. Ohno H. Intestinal M cells. J Biochem. 2016;159(2):151-60.

33. Foster N, Macpherson GG. Murine cecal patch M cells transport infectious prions in vivo. J Infect Dis. 2010;202(12):1916-9.

34. Miller H, Zhang J, Kuolee R, Patel GB, Chen W. Intestinal M cells: the fallible sentinels? World J Gastroenterol. 2007;13(10):1477-86.

35. Ford MJ, Burton LJ, Morris RJ, Hall SM. Selective expression of prion protein in peripheral tissues of the adult mouse. Neuroscience. 2002;113(1):177-92.

36. Miyazawa K, Kanaya T, Tanaka S, Takakura I, Watanabe K, Ohwada S, Kitazawa H, Rose MT, Sakaguchi S, Katamine S, Yamaguchi T, Aso H. Immunohistochemical characterization of cell types expressing the cellular prion protein in the small intestine of cattle and mice. Histochem Cell Biol. 2007;127(3):291-301.

37. Bons N, Mestre-Frances N, Belli P, Cathala F, Gajdusek DC, Brown, P. Natural and experimental oral infection of nonhuman primates by bovine spongiform encephalopathy agents. Proc Natl Acad Sci U S A. 1999;96(7):4046-51.

38. Ji Y, Luo X, Yang Y, Dai Z, Wu G, Wu Z. Endoplasmic reticulum stress-induced apoptosis in intestinal epithelial cells: a feed-back regulation by mechanistic target of rapamycin complex 1 (mTORC1). J Anim Sci Biotechnol. 2018;9:38.

39. Kaser A, Blumberg RS. Endoplasmic reticulum stress and intestinal inflammation. Mucosal Immunol. 2010;3(1):11-6.

40. Mabbott NA, Donaldson DS, Ohno H, Williams IR, Mahajan A. Microfold (M) cells: important immunosurveillance posts in the intestinal epithelium. Mucosal Immunol. 2013;6(4):666-77.

41. Tuma P, Hubbard AL. Transcytosis: crossing cellular barriers. Physiol Rev. 2003;83(3):871-932.

42. Bernier-Latmani J, Petrova TV. Intestinal lymphatic vasculature: structure, mechanisms and functions. Nat Rev Gastroenterol Hepatol. 2017;14(9):510-26.

43. Suh SH, Choe K, Hong SP, Jeong SH, Makinen T, Kim KS, Alitalo K, Surh CD, Koh GY, Song JH. Gut microbiota regulates lacteal integrity by inducing VEGF-C in intestinal villus macrophages. EMBO Rep. 2019;20(4):e46927.

44. Jang JY, Koh YJ, Lee SH, Lee J, Kim KH, Kim D, Koh GY, Yoo OJ. Conditional ablation of LYVE-1+ cells unveils defensive roles of lymphatic vessels in intestine and lymph nodes. Blood. 2013;122(13):2151-61.

45. Vetrano S, Borroni EM, Sarukhan A, Savino B, Bonecchi R, Correale C, Arena V, Fantini M, Roncalli M, Malesci A, Mantovani A, Locati M, Danese S. The lymphatic system controls intestinal inflammation and inflammation-associated Colon Cancer through the chemokine decoy receptor D6. Gut. 2010;59(2):197-206.

46. Akesson CP, McGovern G, Dagleish MP, Espenes A, Mc LPC, Landsverk T, Jeffrey M. Exosome-producing follicle associated epithelium is not involved in uptake of PrPd from the gut of sheep (Ovis aries): an ultrastructural study. PLoS One. 2011;6(7):e22180.

47. Ichikawa S, Kasahara D, Iwanaga T, Uchino S, Fujita T. Peptidergic nerve terminals associated with the central lacteal lymphatics in the ileal villi of dogs. Arch Histol Cytol. 1991;54(3):311-20.

48. Ichikawa S, Kyoda K, Iwanaga T, Fujita T, Uchino S. Nerve terminals associated with the central lacteal lymphatics in the duodenal and ileal villi of the monkey. Acta Anat (Basel). 1993;146(1):14-21.

49. Macpherson AJ, Smith K. Mesenteric lymph nodes at the center of immune anatomy. J Exp Med. 2006;203(3):497-500.

50. O'Connor T, Aguzzi A. Prions and lymphoid organs: solved and remaining mysteries. Prion. 2013;7(2):157-63.

51. Lawson VA, Collins SJ, Masters CL, Hill AF. Prion protein glycosylation. J Neurochem. 2005;93(4):793-801.

52. Lehmann S, Harris DA. Blockade of glycosylation promotes acquisition of scrapie-like properties by the prion protein in cultured cells. J Biol Chem. 1997;272(34):21479-87.

53. Petersen RB, Parchi P, Richardson SL, Urig CB, Gambetti P. Effect of the D178N mutation and the codon 129 polymorphism on the metabolism of the prion protein. J Biol Chem. 1996;271(21):12661-8.

Supplementary Material

The Supplementary Material is available at: http://serbiosoc.org.rs/NewUploads/Uploads/Balcan%20et%20al_5658_Supplementary%20Material.pdf